Multidimensional Estimation of Spectral Sensitivities

Eric Walowit[1], Holger Buhr[2], Dietmar Wüller[2]
[1]Lake Tahoe, California, USA, RikWalowit@aol.com
[2]Image Engineering GmbH & Co. KG, Augustinusstraße 9d, 50226 Frechen, Germany

Abstract

An important step in the color image processing pipeline for modern digital cameras is the transform from camera response resulting from scene spectral radiance to objective colorimetric or related quantities. Knowledge of the camera spectral sensitivities is essential for building robust camera transforms for arbitrary capture and viewing conditions. Monochromator-based techniques are well-known but are cumbersome, slow, and impractical for routine use such as production-line camera calibration. It has been shown that with suitable characterization data it is possible to accurately estimate spectral sensitivities without the use of a monochromator. However, these methods are inherently highly metameric and the performance on likely scene capture spectra is unclear. In the current work, it is shown that combining highly-dimensional characterization data with multidimensional analysis of typical camera responses produces spectral sensitivity estimates for a test camera that performs extremely well on likely scene spectra while minimizing the opportunity for camera observer metamerism.

Introduction

The spectral sensitivities of an imaging system describe the quantum efficiency response to radiation of a given wavelength over the range of all wavelengths which the imaging system can detect. In the case of a typical digital camera, knowledge of the camera spectral sensitivities can be combined with likely scene spectral radiances to build camera-specific color transforms.

Typically, ground-truth measurements of spectral sensitivities are measured with a laboratory-grade monochromator. This requires skilled operators to participate in a time-consuming and expensive process utilizing a monochromator with sufficient power throughput to achieve adequate signal to noise levels as the monochromator is stepped through all wavelengths of interest.

Recently, abbreviated methods have been introduced that allow rapid estimation of spectral sensitivities without the use of a monochromator. These methods present a set of relatively broadband spectral radiances to the camera and the camera responses are recorded. Estimated spectral sensitivities are then numerically optimized from the spectral radiances and the camera responses using a variety of techniques and supporting data.

Related Work

An application [1] for rapid individual calibration of a sample representative of a larger population of similar cameras takes advantage of the fact that the typical spectral sensitivities are already known. Based on *a priori* knowledge of the average spectral sensitivities, a set of spectral radiances from light emitting diodes of well-chosen peak wavelengths and spectral power distributions are presented to the camera and the camera responses are recorded. Constrained singular value decomposition is then used to estimate the spectral sensitivities of the sample camera. While applicable for the intended use-case, generalizing it for arbitrary cameras is problematic since the optimal set of spectral radiances depends somewhat on the camera to be characterized and the robustness of the numerical method when applied to wide sets of cameras from different populations.

The eigenvector method [2] is based on the assumption that most modern digital cameras share similar spectral sensitivity characteristics. With this technique, a monochromator is used to create a database of spectral sensitivities of a variety of makes and models of cameras. The first few (most significant) eigenvectors of the database are computed. Then an illuminated color chart of known spectral reflectances is presented to a test camera whose unknown spectral sensitivities are to be estimated and the camera responses are recorded. The unknown spectral sensitivities are estimated by computing the relative amounts of the eigenvectors that, when combined with the chart spectral radiances, best reproduce the test camera responses. The method produces reasonable spectral sensitivity estimates but since the color chart reflectances used to characterize the camera are of low-dimensionality, the estimated spectral sensitivities are also of low-dimensionality often resulting in estimates that are unable to reliably predict important spectral characteristics. A variation [3] illuminates the reflective chart with a spectrally-tunable light source to increase the dimensionality of the characterization data. However, this adds significant complexity to the characterization setup and achieving high signal levels can be a challenge.

Current Method

In the current approach, the most desirable attributes of the foregoing related work are utilized while avoiding their limitations with a simple setup that lends itself to rapid and reliable spectral sensitivity estimation:

1. An integrating sphere with an internal LED module is used to uniformly illuminate a diffusion plate located in an aperture on the surface of the sphere. The LEDs are of known spectral power distributions and are selected such that the set of peak wavelengths cover the visible spectrum.
2. Each LED illuminates the diffusion plate sequentially and the response of the test camera (whose unknown spectral sensitivities are to be estimated) to each LED are recorded as the characterization data.
3. A database of spectral sensitivities representative of relevant cameras is either measured or obtained.
4. The eigenvectors and their relative contributions to the spectral sensitivity database are determined.
5. The solution is computed for the estimated spectral sensitivities, which relates the relative amounts of each eigenvector that when integrated with the LED spectral power distributions best reproduce the camera characterization data.

Background

While more comprehensive techniques are generally preferred, the current approach is simplified by initially making the following assumptions and revisiting them later:

1. The color sensing behavior of the camera is linear, spatially stationary, and at the time of characterization that setup and exposure is performed in such a manner that noise may be ignored.
2. Each color sensing channel is independent of the others thereby allowing separable estimation of each color channel spectral sensitivity.
3. Cameras do not obey the Luther condition in that their spectral sensitivities are not linear combinations of human color matching functions. Therefore, different characterization data sets and numerical optimization techniques will potentially produce different spectral sensitivity estimates that are approximately metameric with each other and to the actual spectral sensitivities.
4. The estimation procedure may be constrained to produce positive spectral sensitivity estimates at all wavelengths.
5. Scaling the relative heights of the estimated spectral sensitivities can be accomplished by including reference whites in the characterization data set thereby permitting the use of the scaled spectral sensitivity databases.

Given these initial assumptions, camera color formation for each color channel is given by:

$$\mathbf{c} = \mathbf{s}^t\mathbf{T} \tag{1}$$

where **T** is a column matrix of spectral radiances (*e.g.* training or test data) presented to the camera whose dimensions are *i* wavelengths by *j* spectral radiance samples. **s** is a *i*-length vector of the actual spectral sensitivity of the camera for a given color channel. **c** is the resulting vector of camera responses for the given color channel.

The goal is to estimate **e**, the unknown spectral sensitivity for a test camera color channel:

$$\mathbf{c} = \mathbf{e}^t\mathbf{T} \tag{2}$$

T is often comprised of spectral samples that are highly correlated and therefore not linearly independent. Since direct inversion of **T** to estimate **e** is not full-rank, noise-sensitive, poorly-conditioned, and problematic for many reasons, **e** may be estimated instead by determining *k* weights **w** of a selected set of *ixk* most significant eigenvectors **P**:

$$\mathbf{e} = \mathbf{w}^t\mathbf{P}^t \tag{3}$$

so:

$$\mathbf{c} = \mathbf{w}^t\mathbf{P}^t\mathbf{T} \tag{4}$$

then:

$$\mathbf{w} = \mathbf{c}^t(\mathbf{P}^t\mathbf{T})^t[(\mathbf{P}^t\mathbf{T})(\mathbf{P}^t\mathbf{T})^t]^{-1} \tag{5}$$

therefore, the spectral sensitivity estimate **e** reduces to:

$$\mathbf{e} = \mathbf{P}(\mathbf{P}^t\mathbf{T}\mathbf{T}^t\mathbf{P})^{-1}\mathbf{P}^t\mathbf{T}\mathbf{c} \tag{6}$$

and the resulting minimum norm solution for the unknown spectral sensitivity **e** is repeated or extended for all test camera color channels of interest.

Results and Discussion

A recent test camera was characterized by measuring spectral sensitivities directly [4] and by using the estimation technique just described then comparing the results. The legacy database of [2] is employed. Different sets of eigenvectors extracted from the database are evaluated for significance, optimum estimation performance in terms of spectral mismatch, camera RGB prediction accuracy, and noise propagation. Camera RGB prediction accuracy was determined with a set of 2000 spectral radiances representative of actual scene elements, measured in-situ [5] with a telespectroradiometer and substituted for **T** in equations (1) and (2). This is preferred to using chart-based evaluation methods since the spectral basis functions of scenes can be quite different from those of charts. The estimation technique was performed separately using a reflective chart [2] and an LED device [6] to characterize the test camera and the results are compared.

Figure 1 shows that the selected set of cameras show a great deal of similarity in the behavior of their spectral sensitivities. In [2] it was concluded that this behavior is essentially two-dimensional as utilizing only the first two eigenvectors of Figure 2 accounts for more than 97% of the variation shown in Table 1. Nearly all of the variation is accounted for in the first four eigenvectors.

Two-dimensional estimation allows for the use of the reflectance color chart of Figure 3a as spectral radiances for **T** to obtain camera responses **c** since Figure 3b and Table 2 suggest adequate dimensionality in the characterization data for this purpose. The first two eigenvectors account for nearly all the variation in the chart reflectances. However, Figure 5a shows that including only two dimensions does not completely predict the actual spectral sensitivity behavior of the test camera. Furthermore, Table 3 - Chart shows that including higher-order eigenvectors does not lead to better prediction accuracy since estimating the weights of additional higher-dimensional eigenvectors is not well-determined due to the relatively low-dimensionality of the color chart reflectances.

In order to increase prediction accuracy, higher dimensionality in the characterization data, **T** and **c**, is required if additional higher-dimensional eigenvectors are to be included in the solution. Figure 4 and Table 2 show the spectral power distributions and dimensionality characteristics of the LED device used for this purpose. The first four eigenvectors of the LED spectral power distributions account for just three-fourths of the variation. In the current work, the full set of LEDs are included but as a practical matter, a well-chosen subset can be selected, especially if insight into the generic spectral sensitivity characteristics of cameras to be estimated has already been gained.

Figure 5 compares results obtained by including the first four eigenvectors when solving for **e** using the LED-based characterization data versus the chart-based method. It can be seen that the estimated spectral sensitivities more closely match the measured ones and that the prediction errors have fallen significantly. Table 3 - LED shows that including higher-order eigenvectors produces better prediction accuracy since estimating the weights of additional higher-dimensional eigenvectors is improved by the higher-dimensionality of the LED spectra.

However, since the narrow-band grating-type monochromator used to create the database is very different from the abridged filter-based instrument used to measure the reference spectral sensitivities of the test camera, some errors can be expected and

are built in to Table 3. In practical applications, all monochromator measurements should be made with the same instrument.

It can be useful to visualize the actual and estimated red and green spectral sensitivities in terms of the camera locus:

$$\mathbf{l}(r,g) = (\mathbf{e}(r)/(\mathbf{e}(r)+\mathbf{e}(g)+\mathbf{e}(b),\mathbf{e}(r)/(\mathbf{e}(r)+\mathbf{e}(g)+\mathbf{e}(b)) \quad (7)$$

Figure 6 compares the shape and behavior of the spectral loci predictions from both sets of characterization data with that determined from the measured spectral sensitivities. The LED-based higher-dimensional estimation results match the expected behavior much more closely.

While it was assumed that at the time of characterization that noise effects were negligible and no noise term was included in the estimation model, it is useful to observe noise propagation effects that simulate application of the estimation transform as applied to scene data with a simple noise percentage (n) model:

$$\mathbf{c}_n = \mathbf{e}^t\mathbf{T}+n \quad (8)$$

or:

$$\mathbf{e}_n = \mathbf{P}(\mathbf{P}^t\mathbf{T}\mathbf{T}^t\mathbf{P})^{-1}\mathbf{P}^t\mathbf{T}(\mathbf{c}+n) \quad (9)$$

Figure 7 shows the errors resulting from adding varying percentages of noise to the signal. At reasonable noise levels, the LED-based 4-dimensional estimation procedure compares favorably with the 2-dimensional chart-based method.

It is important to recognize that these methods produce spectral sensitivity estimates that are inherently metameric with each other and potentially metameric with the actual spectral sensitivities in the following sense. Suppose **E** is a column matrix of the full set of exactly-determined estimated spectral sensitivities and **S** is a column matrix of the known spectral sensitivities. Further suppose **C** is a set of camera response values (*e.g.* RGB) to a set of spectra **T** used to exactly-determine **E**. Then:

$$\mathbf{E}^t\mathbf{T} = \mathbf{C} = \mathbf{S}^t\mathbf{T} \quad (10)$$

producing the result that the estimated spectral sensitivities are observer-metameric with the actual ones, where the observer in this case is the camera.

Now further suppose **O** is a set of CIE-observer tristimulus values (*e.g.* XYZ) of some spectra used to exactly-determine camera color transforms m_1 (from **E** and **O**) and m_2 (from **S** and **O**). Then:

$$m_1\mathbf{E}^t\mathbf{T} = \mathbf{O} = m_2\mathbf{S}^t\mathbf{T} \quad (11)$$

Since both products yield the same tristimulus values they are metameric to each other. Different methods and characterization data sets that are optimized for the same tristimulus values may also produce products of m and **E** that are metameric with each other and with the CIE standard observer. Colors that look different to a human may reproduce as the same color after applying equation (11) and vice-versa.

Typically, the various transforms and estimates are computed in an overdetermined manner, so the results can be considered to be approximately metameric in a least-squares sense. Since the current method produces spectral sensitivity estimates that closely approximate the actual spectral sensitivities, potential metameric issues between the two sets are minimized.

Conclusions

A simple setup and method was developed to rapidly characterize current cameras for the purpose of accurately and robustly estimating spectral sensitivities without the use of a monochromator. The dimensionality of the characterization data is sufficiently high to allow use of higher-order eigenvectors extracted from a legacy database of spectral sensitivities measured with a monochromator. This is an improvement over previous approaches which require either more complicated setups or are limited to less accurate estimation methods.

References

[1] J. M. DiCarlo, G.E. Montgomery, and S.W. Trovinger, "Emissive chart for imager calibration," in Twelfth Color and Imaging Conference: Color Science and Engineering, Scottsdale, Arizona, 2004.

[2] J. Jiang, D. Liu, J. Gu, and S. Susstrunk, "What is the space of spectral sensitivity functions for digital cameras?," in IEEE Workshop on Applications of Computer Vision, Tampa, Florida, 2013.

[3] T.M. Tanksdale and P. Urban, "Trichromatic reflectance capture using a tunable light source: setup, characterization and reflectance estimation," in IS&T International Symposium on Electronic Imaging: Measuring, Modeling, and Reproducing Material Appearance, San Francisco, California, 2016.

[4] Image Engineering GmbH &Co. KG, Frechen, Germany, "camSPECS express v2 Measurement Device".

[5] D. Wüller, "In situ measured spectral radiation of natural objects," in Seventeenth Color and Imaging Conference: Color Science and Engineering Systems, Technologies, and Applications, Albuquerque, New Mexico, 2009.

[6] Image Engineering GmbH &Co. KG, Frechen, Germany, "Cal1 Calibration light source".

Author Biography

Eric Walowit's interest is in appearance estimation, color management, camera characterization, and digital photography. He is founder (retired) of Color Savvy Systems, a color management company. He currently helps friends and colleagues with interesting color problems and ventures. He graduated from RIT's Image Science program in 1985, concentrating in Color Science. He has authored more than 50 patents, publications, and presentations. Eric is a member of ICC, ISOTC42, and IS&T.

Dietmar Wüller studied photographic sciences from 1987 to 1992 in Cologne. He is the founder of Image Engineering, a leading supplier of test equipment for digital image capture devices. He is a member of IS&T, DGPH, and ECI. Dietmar is the German representative for ISO TC42 WG18 and also participates in several other standardization activities.

Holger Buhr is a software engineer with Image Engineering. He graduated from the Cologne University of Applied Sciences (CUAS) in photographic science in 2006. He worked as a scientific coworker at the CUAS in the domain of radiological imaging and computer science.

The authors wish to acknowledge Michael Vrhel and Harold Boll for their helpful comments.

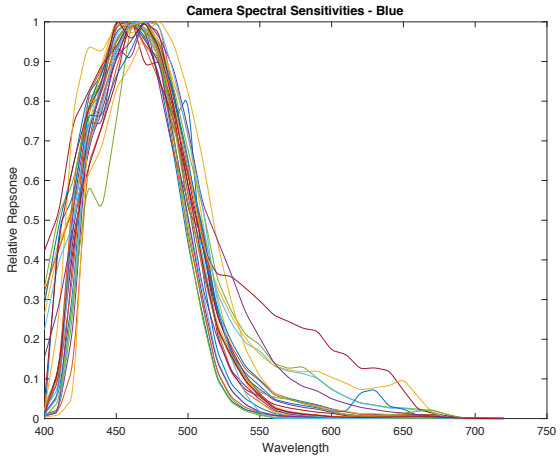

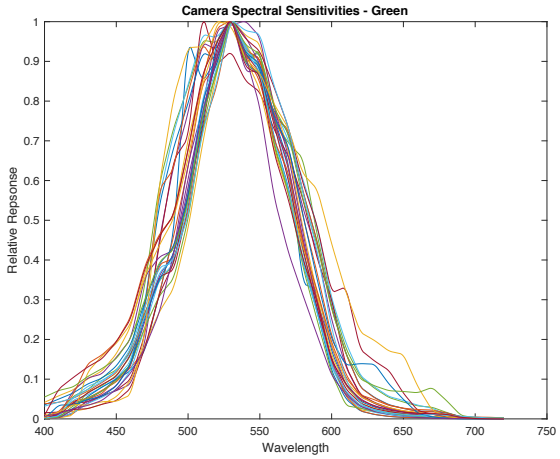

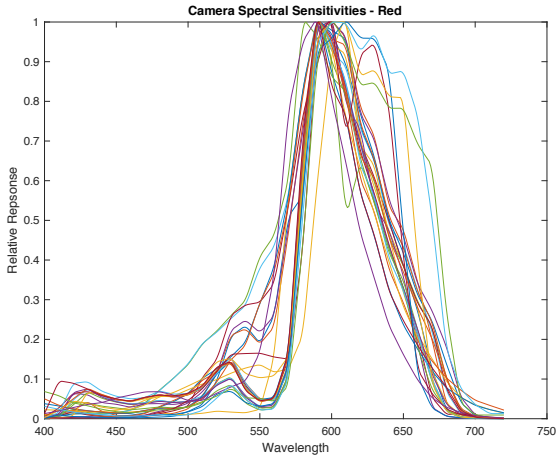

Figure 1. *Scaled monochromator-measured spectral sensitivity database for 28 legacy cameras*

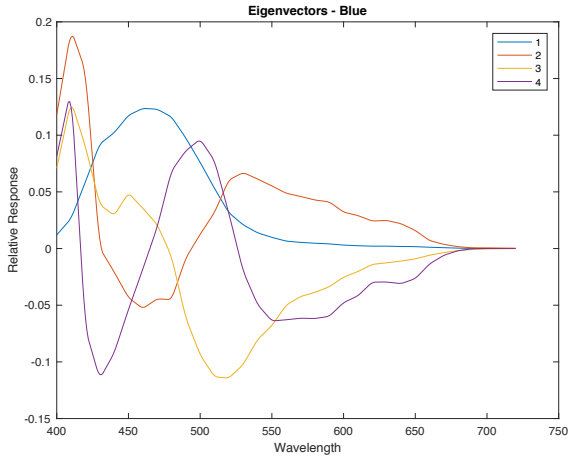

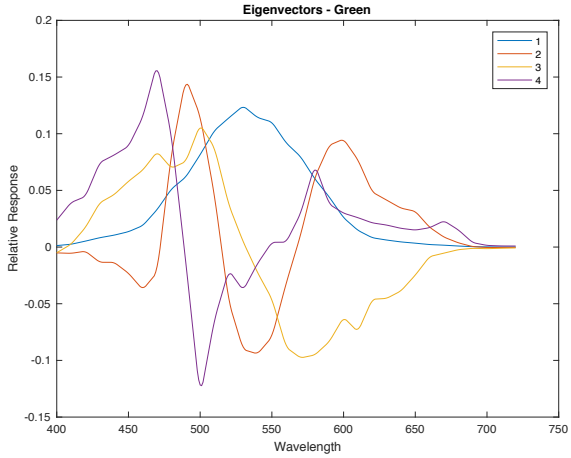

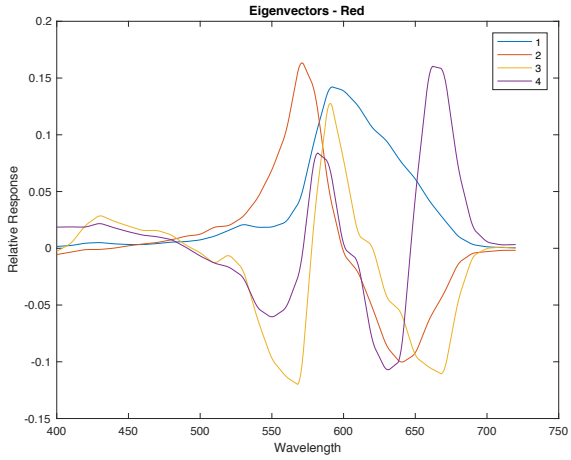

Figure 2. *First 4 eigenvectors of the spectral sensitivity database*

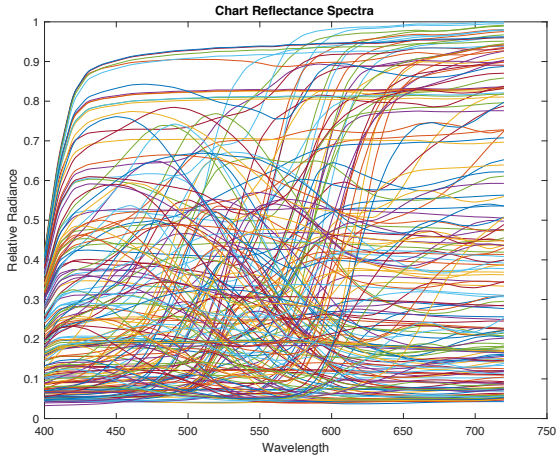

Figure 3a. *Chart spectral reflectance*

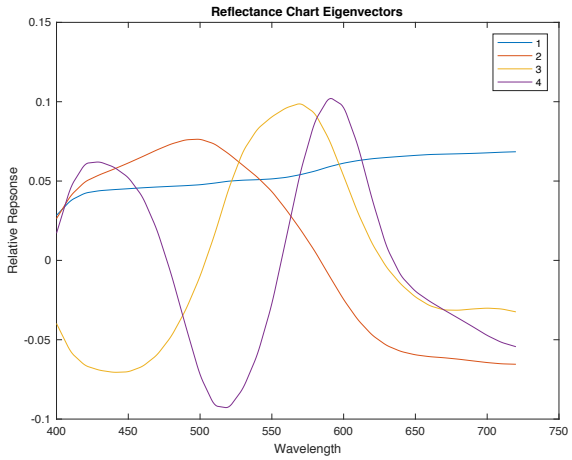

Figure 3b. *First 4 eigenvectors of the reflective chart*

Table 1: Camera spectral sensitivity database relative eigenvector cumulative contribution percentages

EVs	R	G	B
1	95.6	98.8	98.0
2	97.8	99.4	98.9
3	98.9	99.7	99.4
4	99.4	99.8	99.7

Table 2: Characterization data sets relative eigenvector cumulative contribution percentages

EVs	Chart	LED
1	90.2	31.9
2	97.7	49.6
3	99.4	62.9
4	99.7	73.2

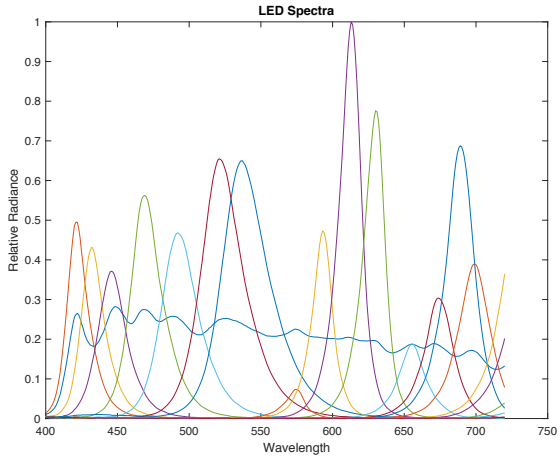

Figure 4a. *LED spectral power distributions*

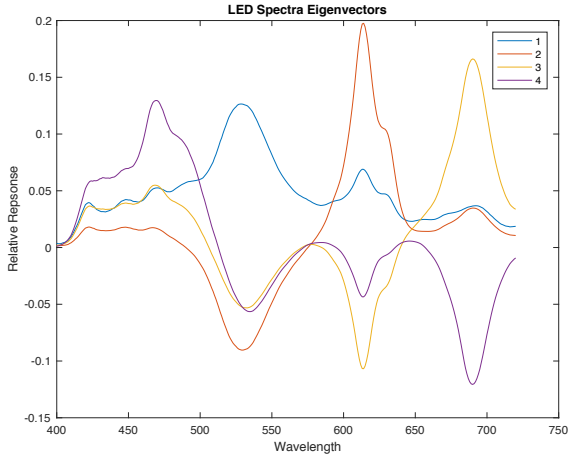

Figure 4b. *First 4 eigenvectors of the set of LEDs*

Table 3: Errors for chart-based and LED-based spectral sensitivity estimation methods for the test camera

EVs	Chart			LED		
	RMS	*Ave % RGB Error*	*Max % RGB Error*	*RMS*	*Ave % RGB Error*	*Max % RGB Error*
1	.056	0.23	2.58	.055	.23	2.58
2	.081	0.28	4.23	.048	.19	2.65
3	.089	0.38	3.83	.047	.11	2.81
4	.520	1.13	34.6	.040	.09	2.10

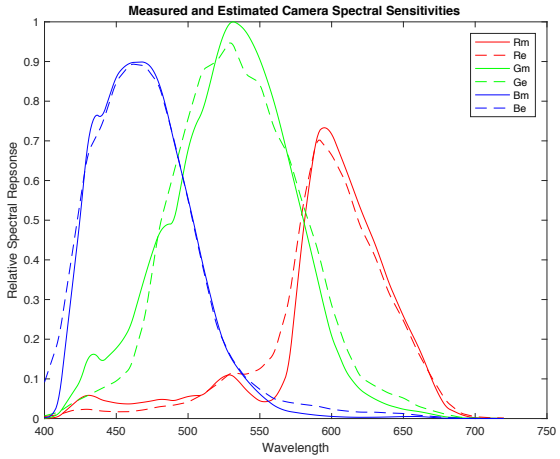

Figure 5a. *Measured and chart-based spectral sensitivity estimates for test camera*

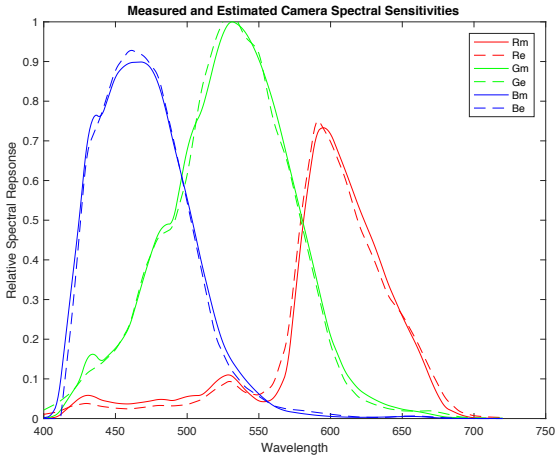

Figure 5b. *Measured and LED-based spectral sensitivity estimates for test camera*

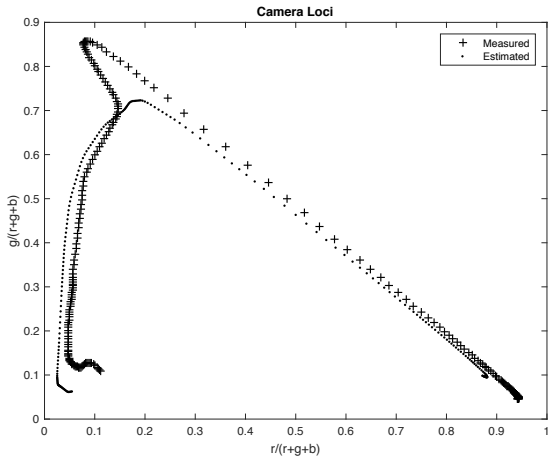

Figure 6a. *Measured and chart-based camera loci predictions for the test camera*

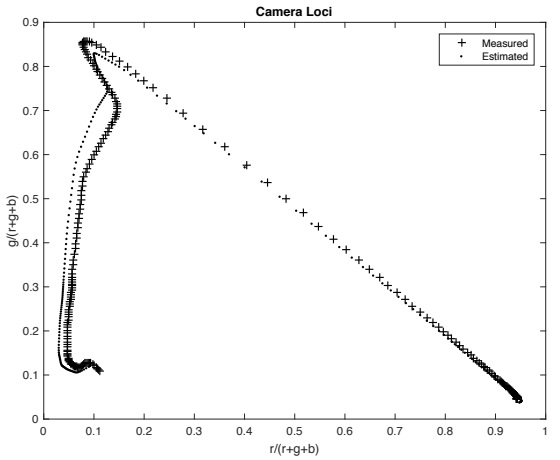

Figure 6b. *Measured and LED-based camera loci predictions for the test camera*

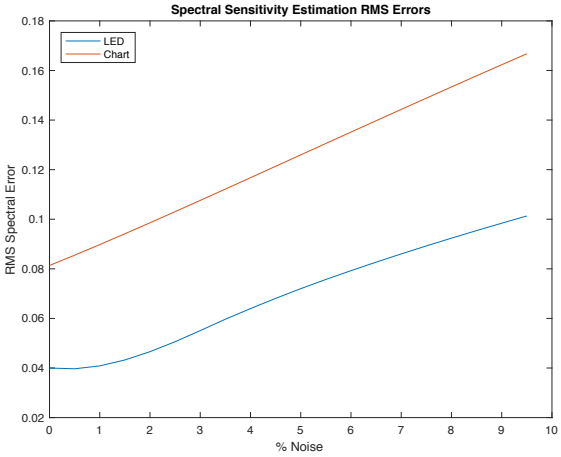

Figure 7a. *Spectral sensitivity estimation RMS errors for increasing noise levels for the test camera*

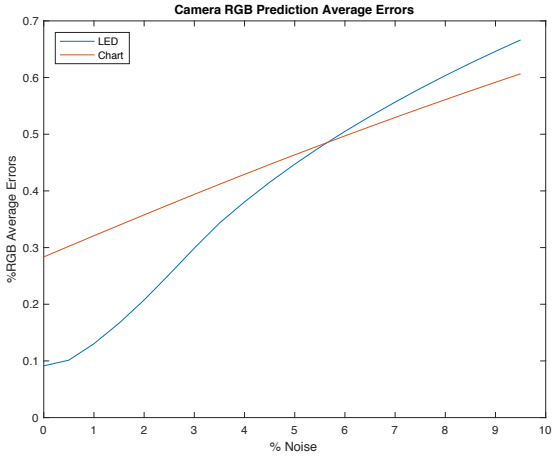

Figure 7b. *Average camera RGB prediction errors for increasing noise levels for the test camera and in situ test spectra*